Custom Coordination Environments for Lanthanoids: Tripodal Ligands Achieve Near-Perfect Octahedral Coordination for Two Dy-Based Molecular Nanomagnets

Kwang Soo Lim,[†,&] José J. Baldoví,[⊥,&] ShangDa Jiang,[‡,§,&] Bong Ho Koo,[†] Dong Won Kang,[†] Woo Ram Lee,[†] Eui Kwan Koh,[∥] Alejandro Gaita-Ariño,*[,⊥] Eugenio Coronado,[⊥] Michael Slota,[‡] Lapo Bogani,*[,‡] and Chang Seop Hong*[,†]

[†] Department of Chemistry, Korea University, Seoul 136-713, Republic of Korea.
[⊥] Instituto de Ciencia Molecular (ICMol), Universidad de Valencia, C/Catedrático José Beltrán, 2, E-46980 Paterna, Spain.
[‡] Department of Materials, University of Oxford, 16 Parks Road, OX1 3PH, Oxford, UK.
[§] Inorganic Chemistry, College of Chemistry and Molecular Engineering, Peking University, Beijing 100871, P.R. China.
[∥]Nano-Bio System Research Team, Korea Basic Science Institute, Seoul 136-713, Korea.

Keywords: single-ion magnets, lanthanides, crystal-field theory, magnetic anisotropy.

Supporting Information Placeholder

ABSTRACT: Controlling the coordination sphere of lanthanoid complexes is a challenging critical step towards controlling their relaxation properties. Here we present the synthesis of hexa-coordinated Dy single-molecule magnets where tripodal ligands achieve a near-perfect octahedral coordination. We perform a full experimental and theoretical investigation of their magnetic properties, including a full single-crystal magnetic anisotropy analysis. The combination of electrostatic and crystal field computational tools (SIMPRE and CONDON codes) allows explaining the static behaviour of these systems in detail.

Introduction.

Since the first observation of slow magnetic relaxation in mononuclear lanthanide complexes $[Pc_2Ln]^-$ (Pc = phthalocyanide, Ln^{III} = Tb, Dy, Ho),[1] the field of mononuclear single-ion magnets (SIMs) and molecular spin qubits has expanded significantly, and now includes multiple examples based on either lanthanoids or transition metals, or even actinoids.[2] Considered as classical bistable systems, they have set record values for the temperatures at which slow relaxation of the magnetization sets in. More interestingly, their quantum properties make them very attractive as spin qubit systems.[3] Recently, record relaxation times have been obtained in transition metal complexes, where there is a greater control over the coordination sphere.[4] Moreover, in the quest for longer relaxation times at higher temperatures, different authors are now insisting on the need of exerting some control over the molecular vibrations and not only focusing on the thermal barrier.[2b, 5] The physics behind these arguments shares common ground for both transition-metal and lanthanoid complexes, but the chemical control of the coordination sphere is different. This is primarily due to the differences between *d* and *f* orbitals (the latter being more internal) and, secondarily, to the larger coordination sphere and higher coordination number of the lanthanoids. Attempts to address this problem have been performed by the use of rigid and bulky ligands such as polyoxometalates.[6] Still, the full validation of theoretical models and the

creation of a common background that can relate the rare-earth magnetism to the ligand-field analysis is largely unexplored.[7]

Dy^{III}, in particular, has seen much use in the design of single-molecule magnets (SMMs), because of its high magnetic anisotropy.[8] In sandwich-type structures, Dy^{III} complexes should theoretically display strong axial anisotropy along the sandwich axis, but experiments show substantial deviations from these predictions. Despite insight obtained from octa-coordinated Dy complexes with square antiprismatic geometries, where the properties can be adjusted by local symmetry distortions and ligand substitution,[9] the lack of model systems and of treatable situations is substantial. It has also been noted that special symmetries such as the octahedron or the cube can give rise to unique quantum properties. As discussed previously by Baldoví et al,[10] the abundance of degenerate or near-degenerate electronic spin energy levels, even prior to the consideration of nuclear spins, creates a wealth of opportunities for avoided crossings and therefore for Clock Transitions (CTs), which can be used for improved quantum coherence as we illustrated recently.[11] Furthermore, even in absence of CTs, a sufficiently large number of spin states in an accessible energy window can be used to construct multi-qubit (or d-bit) systems where coherent transitions are demonstrated.[12]

Compared to Dy-based magnetic systems with coordination numbers larger than 7, a six-coordinate Dy complex (not cluster) is rarely known[13,14] and highly sought to further understand fundamental magnet-like behaviors. Here we present the synthesis, structure, and magnetic properties of Dy SMMs in custom-shaped and uncommon octahedral coordination, providing model compounds for the understanding of rare-earth magnetism.

Materials and Methods.

Reagents. All chemicals and solvents in the synthesis were reagent grade and used as received. $Na[CpCo\{P(O)(OEt)_2\}_3]$ (NaL_{OEt}) and $Na[CpCo\{P(O)(OiPr)_2\}_3]$ (NaL_{OiPr}) were prepared according to literature procedures.[15]

$[Dy(L_{OEt})_2](PF_6)$ (1): NaL_{OEt} (55.7 mg, 0.10 mmol) and NH_4PF_6(16.3 mg, 0.10 mmol) were dissolved in water (15 mL) and stirred for 10 min. A yellow precipitate was generated immediately upon addition of $Dy(NO_3)_3 \cdot 5H_2O$ (17.4 mg, 0.05 mmol) in water (2 mL) to the ligand solution. The mixture was stirred for 12 h and the precipitate was filtered and washed with water. Vapor diffusion of diethyl ether into a methanol solution yielded crystals suitable for X-ray analysis. Yield: 52.1 mg (75.6%). Anal. calcd for $C_{34}H_{70}Co_2DyF_6O_{18}P_7$: C, 29.62; H, 5.12. Found: C, 29.62; H, 5.04.

$[Y(L_{OEt})_2](PF_6)$: The Y analogue was obtained by the same procedure as for compound **1**, except that $Y(NO_3)_3 \cdot 6H_2O$ was used instead of Dy(III). Yield: 72.3%. Anal. Calcd for $C_{34}H_{70}Co_2YF_6O_{18}P_7$: C, 31.30; H, 5.41. Found: C, 31.38; H, 5.49.

$[Dy(L_{OEt})_2](PF_6)$ diluted 20-fold with $[Y(L_{OEt})_2](PF_6)$ (diluted-1): An aqueous solution (2 mL) of $Dy(NO_3)_3 \cdot 5H_2O$ (0.005 mmol) and $Y(NO_3)_3 \cdot 6H_2O$ (0.10 mmol) was added to a solution of NaL_{OEt} (111.4 mg, 0.20 mmol) and NH_4PF_6(32.6 mg, 0.20 mmol) in water (15 mL) with stirring. A yellow precipitate was generated and the mixture was stirred at room temperature for 12 h. The precipitate was filtered, washed with water and dried in air. Anal. Calcd for $C_{714}H_{1470}Co_{42}Y_{20}DyF_{126}O_{378}P_{147}$: C, 31.22; H, 5.39. Found: C, 31.33; H, 5.35.

$[Dy(L_{OiPr})_2](PF_6)$ (2): Compound **2** was obtained by the same procedure as for compound **1** except for using NaL_{OiPr} instead of NaL_{OEt}. Yield: 52.7%. Anal. Calcd for $C_{46}H_{94}Co_2DyF_6O_{18}P_7$: C, 35.77; H, 6.00. Found: C, 35.77; H 6.08.

Physical Measurements. Elemental analyses for C, H, and N were performed at the Elemental Analysis Service Center of Sogang University. PXRD data were recorded using Cu Kα (λ = 1.5406 Å) on a Rigaku Ultima III diffractometer with a scan speed of 2°/min and a step size of 0.02°. Magnetic susceptibilities for complexes **1** and **2** were carried out using a Quantum Design SQUID susceptometer (dc) and a PPMS magnetometer (ac). Diamagnetic corrections of all samples were estimated from Pascal's Tables.

Crystallographic Structure Determination. X-ray data for **1** and **2** were collected on a Bruker SMART APEXII diffractometer equipped with graphite monochromated MoKα radiation (λ = 0.71073 Å). Preliminary orientation matrix and cell parameters were determined from three sets of ϕ scans at different starting angles. Data frames were obtained at scan intervals of 0.5° with an exposure time of 10 s per frame. The reflection data were corrected for Lorentz and polarization factors. Absorption corrections were carried out using SADABS. The structures were solved by direct methods and refined by full-matrix least-squares analysis using anisotropic thermal parameters for non-hydrogen atoms with the SHELXTL program. In complex **2**, the Cp ring and di-isopropyl-phosphito groups were disordered over two sites (0.61: 0.39 for parts A and B, respectively) using PART and isopropoxy groups were isotropically refined. All hydrogen atoms were calculated at idealized positions and refined with the riding models. Crystal data for **1** and **2** are summarized in Table S1.

Computational Details. The electronic structures of **1** and **2** were determined using the CONDON computational package.[16] As starting point, we have used the crystal-field parameters (CFPs) determined by the REC model[17] using the SIMPRE computational package[18] and assuming an ideal D_{3d} coordination environment with the C_3 axis oriented in z. Then, the magnetic properties of **1** were fitted using the full Hamiltonian. The resulting CFPs were tested with the prediction of the experimental single-crystal magnetic anisotropy measurements. Due to the chemical and structural similarity of **2**, the set of CFPs determined for **1** was used as input to fit the magnetic properties of **2**. The free-ion parameters of Dy introduced in CONDON (electron repulsion parameters: F^k (k = 2,4,6) and spin-orbit coupling constant: ξ_{SO}) were not varied during the fitting procedures.

Results and discussion

Description of the Structures. To design the complexes we chose the tripodal ligands $[CpCo[P(O)(OR)_2]_3]^-$ (Figure S1) here shortened in L_{OR}^- (R=Et, *i*Pr), because huge steric encumbrance is fundamental to hinder the tendency of rare-earths to higher coordination numbers (synthesis in the experimental section). Both $[Dy(L_{OR})_2]^+$ complexes crystallize in the monoclinic space group *C*2/*c*, with a PF_6^- anion (Figure 1).

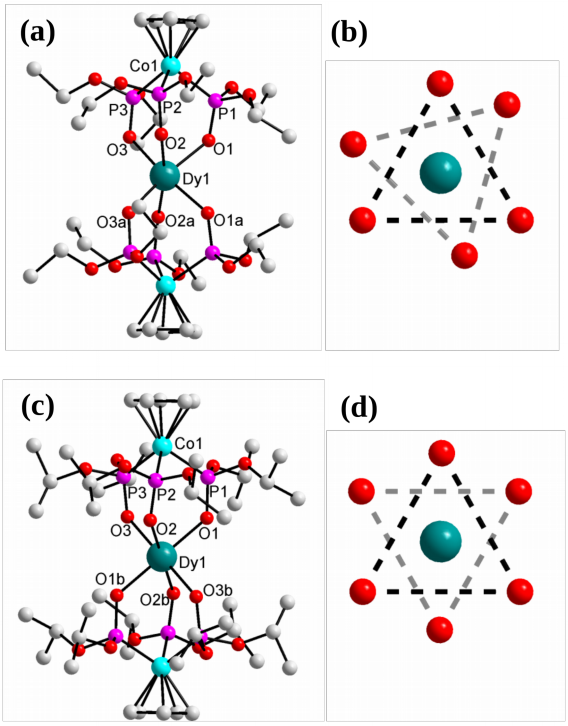

Figure 1. View of the crystal structure of: (a) The cationic part of **1**, and (b) its Dy coordination environment. (b); (c) The cationic part of **2**, and its Dy coordination environment (d). Hydrogen atoms are omitted for clarity.

The Dy atom is sandwiched between 6 oxygens from two L_{OR}^- ligands, successfully forming the planned hexa-coordinate structure. The Dy-O bond lengths are very homogeneous, ranging between 2.249 and 2.257 Å for **1** and between 2.246 and 2.265 Å for **2**. The angular deviation parameter, defined as sum of the deviation from 90° of the 12 *cis* angles in the coordination sphere, is estimated to be Σ=90.9° for **1** and 71.6° for **2**.[19] The shape-deviation parameters S_X against an ideal octahedron (X=O) and a trigonal prism (X=P) provides S_O=1.66, S_P=8.95 for **1**, and S_O=0.52 and S_P=15.11 for **2**, showing that continuous shape measures[20] clearly indicate an octahedral geometry. While a perfect octahedron is obtained in **2**, the use of different L_{OR}^- ligands allows distorting the octahedron, producing a twisting angle in **1** (Figures 1b and 1d). The diamagnetic CpCo and PF_6^- parts are positioned among the molecules and magnetically shield them, with

the shortest Dy-Dy distance is 12.1 Å for **1** and 12.7 Å for **2** (Figures S2 and S3).

Magnetic Properties. The magnetic susceptibilities χ_m of **1** and **2** (i.e. the ratio M/H between the magnetization M and the magnetic field H) were measured at H = 1 kOe down to 2.0 K (Figures S5 and S6). The $\chi_m T$ values at room temperature for **1** and **2** are 13.5 and 13.7 cm^3 K mol^{-1}, respectively, close to the 14.2 cm^3 K mol^{-1} value expected for the $^6H_{15/2}$ state of Dy^{III}. $\chi_m T$ first decreases gradually with T, and plummets abruptly below 40 K, due to depopulation of the Stark sublevels.[21] M vs H (Figures S7 and S8) likewise indicates the presence of strong magnetic anisotropy.[22]

The magnetization dynamics were investigated by measuring the in-phase χ_m' and out-of-phase χ_m" response of the samples under a small field oscillating at frequency ω (Figures 2 and S9 - 23). At H=0 quantum tunneling between degenerate levels leads to very fast relaxation.[23] On increasing H the relaxation time τ becomes slower, reaches a peak (at H_p=600 and 750 Oe for **1** and **2**) and then decreases rapidly, as expected for progressive suppression of quantum tunneling by H. Both **1** and **2** show a frequency dependent peak in χ_m" vs T, and τ was extracted by fitting the ac curves with a Debye model. The resulting Arrhenius plot shows a linear region at high T and a marked kink at lower T, indicating the presence of a thermally-activated mechanism still competing with quantum tunneling.

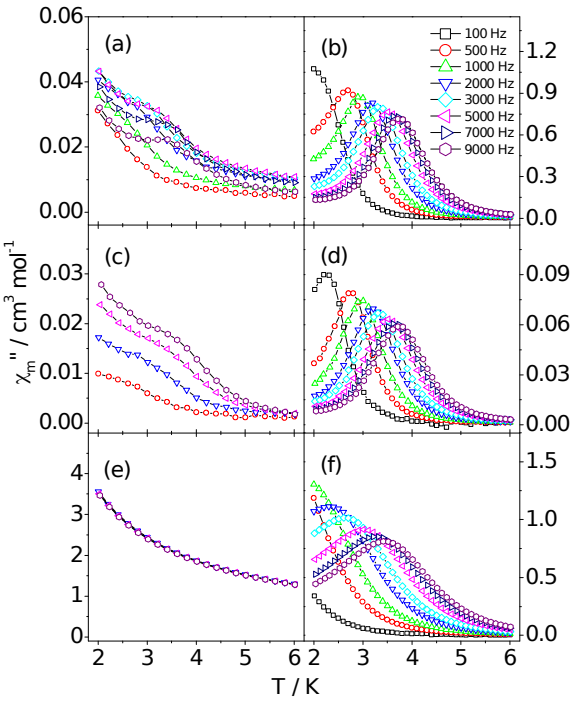

Figure 2. Temperature dependence of out-of-phase component of the ac magnetic susceptibility, χ_m" in zero external field for a) **1**, c) **diluted-1**, and e) **2**, and in the external field H_P where the relaxation is slowest for: b) **1**, H_P = 600 Oe; d) **diluted-1**, H_P = 450 Oe; f) **2**, H_P = 750 Oe.

In order to avoid overparameterization we fit the ac magnetometry data considering either Raman together with quantum tunneling processes (Figure S24) or a simple Orbach-only process (Arrhenius plot), as expressed by the following equation: [24]

$$\tau = \tau_0 \exp(U_{eff}/kT)$$

The fit resulted in τ_0 = 2.4(5) x 10^{-8} s and ΔE = 18(2) cm^{-1} for **1**, and τ_0 = 6.4(5) x 10^{-7} s and ΔE = 9(1) cm^{-1} for **2** (Figure 3). Both τ_0 values are compatible with SMM behaviour, and fitting of the Argand plots (Figures S13 and S18) shows a narrow distribution of relaxation times, with the spreading parameter α=0.2 and 0.1 for **1** and **2**, respectively. Doping with Y^{III} produces a very similar dynamic behaviour, with a slight decrease of H_p to 450 Oe, and longer τ values. The resulting Arrhenius fit provides τ_0 = 6.0(6) x 10^{-9} s and ΔE = 21(2) cm^{-1}. The spin-flip attempt rate roughly matches the expected

value for spin-phonon processes, and a barrier at the limits of the extraction errors.

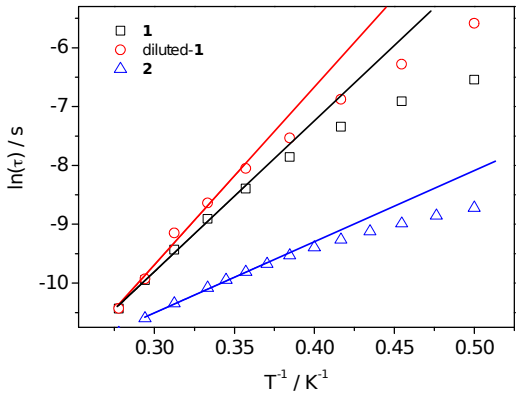

Figure 3. Dynamics of the magnetization as extracted from ac susceptibility measurements for **1** (black squares), **2** (blue triangles) and **1** diluted in a diamagnetic Y^{III} matrix (red circles). The solid lines represent fits from Arrhenius formula.

As seen in Figure 3, a simple Arrhenius plot does not capture all the physics in this system. Raman processes seem to be dominant in the case of **1**, where a satisfactory fit can be obtained for n=9 (Figure S24). The n values of **1** and diluted-**1** are close to 9, consistent with the parameters obtained from the fitting with an additional Orbach process. However, the Raman model fails for **2**. When n is fixed to 9, the fit of **2** is poor.

Single-Ion Anisotropy. We now examine the role of the pseudo-axial local environment of the Dy^{III} octahedron in the anisotropy (Figures S25 – S30). Since, in **1**, the Dy centre is located on a C_2 rotation axis of the C2/c space group, the molecular susceptibility tensor **χ** must coincide with the crystal one and it is possible to obtain the full magnetic anisotropy by rotating around three orthogonal axes in the low-*H* limit (Figure 4a). By a fitting and diagonalization procedure we obtain the orientation and magnitude of the principal axes at different *T*. One eigenvalue is always dominant, with very prominent easy-axis anisotropy oriented along the pseudo C_3 molecular axis (Co-Co direction, Figure 4b). This reveals a clean example of uniaxial behaviour, consistent with expectations from the theory of octahedral transition-metal ions, and without the problems associated to higher-coordination systems. For **2** the same procedure is not possible, as the crystal symmetry prevents a direct extraction of the molecular susceptibility.

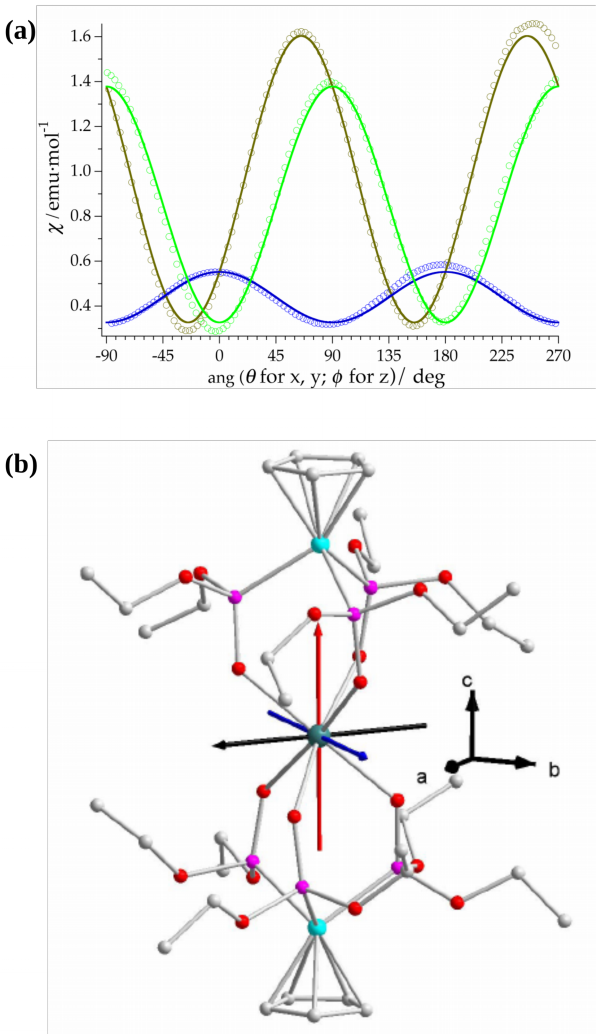

Figure 4. (a) Angular dependence of the magnetic susceptibility of **1** at 11 K. Solid lines are the results of theoretical calculations. (b) Molecular structure showing easy axis direction determined from experiment for easy axis (red), medium axis (blue), and hard axis (black).

Theoretical Calculations. The crystallographic coordinates of the first coordination sphere of **1** were idealized in order to reduce the number of non-negligible CFPs. The molecule was oriented with the pseudo-C_3 main axis pointing in *z*. The idealization of the coordinates resulted in two alternated equilateral triangles of point charges equidistant with respect to the Dy ion (~2.25

Å). An initial individual fit of the powder magnetic susceptibility data using the REC model was performed obtaining the following initial set of CFPs in Wybourne notation (cm^{-1}): B_{20} = 415; B_{40} = -2066; B_{43} = 2070; B_{60} = 432; B_{63} = 2060; B_{66} = 702. They were entered as input in the CONDON package and only two iterations were needed to obtain a very satisfactory fit (SQX = 0.81%, Figure S5) resulting in the following set of CFPs in Wybourne notation (cm^{-1}): B_{20} = 559(84); B_{40} = -3300(283); B_{43} = 1693(51); B_{60} = 450(73); B_{63} = 2034(96); B_{66} = 718(342). Magnetization at 4, 5 and 6 K was also reproduced (Figure S7). According to this description, the first excited Kramers doublet is found at 32 cm^{-1} and the total crystal field splitting of the ground-*J* is about 950 cm^{-1}. The energy levels distribution of the ground-*J* is reported in Table S3. The lowest energy doublet from the next multiplet is located 2668 cm^{-1} above in energy, placed at ~3618 cm^{-1}. The ground Kramers doublet in the easy axis orientation is described by 89.6% of |±11/2> with a 9.4% contribution of |±5/2>, which corresponds to an effective $g_{//}$ of 13.74 ($g_{//}$(exp) = 13.83)) and $g_{\perp}$ = 0.48. This description is almost in perfect agreement with the observed easy-axis behaviour (Figure S29). Thus, the angular dependence of the susceptibility of **1** is also reproduced accurately (Figures S31 – S33), validating once more the theoretical results. Secondly, due to the chemical similarity and similar coordination environment of **2**, we have used the calculated set of CFPs as starting point to model the magnetic susceptibility of **2**. An excellent agreement with SQX = 0.69% (Figure S6) was achieved with the following set of CFPs in cm^{-1}: B_{20} = 467(301); B_{40} = -3605(990); B_{43} = 596(215); B_{60} = 164(133); B_{63} = 1545(281); B_{66} = -357(2489), reproducing also magnetization curves (Figure S8). The uncertainties estimated for the CFPs are reported in Table S2. The large uncertainties found in some of the CFPs likely stem from the sole consideration of powder magnetic susceptibility data, i.e. single-crystal data was not taken into account. One should consider these uncertainties as an upper-limit since (1) we introduced structural information as a starting point and (2) we are predicting instead of fitting the magnetic anisotropy experimental data. The energy level scheme of the ground multiplet is also reported in Table S3. The first excited doublet is placed at about 44 cm^{-1} and the total splitting is ~853 cm^{-1}. In this case, the ground state wave function is more pure, being determined by 98.4% of |±11/2> according to our calculations. This leads to a slightly larger value of $g_{//}$ (14.54) compared with **1** (13.74). Nevertheless, this subtle difference would need a finer determination by spectroscopic measurements.

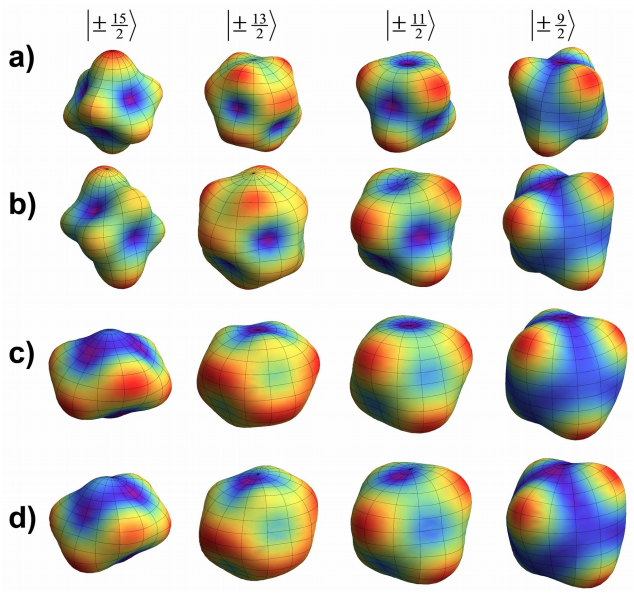

Figure 5. Potential energy surfaces, represented in spherical coordinates, for the different orientations of the pure $|m_j\rangle$ spin sublevels (only the highest four displayed) for: a) **1**; b) **2**; The same plot for **1** (c) and **2** (d) by removing the positive charged and diamagnetic Co^{III} ions. The colorscale indicates the energy (violet lowest and red highest) and the vertical position is along the pseudo-C_3 axis.

In square antiprismatic systems, the dynamics depend on the axial compression or elongation of the complex, and the presence of a twist angle lowers the barrier and introduces additional transverse terms that favour quantum tunneling. We now use an electrostatic model to reproduce the observations and study structure-properties correlations. The states of rare earths are, in general, a linear combination of pure $|m_j\rangle$ spin

sublevels, with mixing introduced by the high spin-orbit coupling and the symmetry of the system. In ligand-field theory the orientation of the quantization axis depends only on the distribution of the charges around the spin. By expanding the electron density of the $|m_j\rangle$ states into a series of spherical harmonics Y_k^0 (with $k \leq 6$),[25] we can calculate the potential energy of each pure $|m_j\rangle$ state as a function of the orientation, so as to find the resulting preferred orientation of the easy-axis. [7] The results obtained considering the charges inside **1** and **2** are plotted in Figures 5a and 5b against the azimuthal φ and polar θ angles of the spherical coordinates. From the results it is evident that, for **1**, both $|11/2\rangle$ the $|9/2\rangle$ states have an absolute energy minimum at θ=0, which corresponds to the direction of the pseudo-C_3 molecular axis. They must thus be the dominant contribution to stabilize the observed orientation of the magnetization easy-axis. This is in perfect agreement with the phenomenological fit by CONDON for both complexes. On the contrary, the highest m_j state, $|15/2\rangle$, often assumed as the dominant ground state contribution in rare-earth SMMs, stabilizes a tilted easy-axis. A more regular octahedral geometry, as observed in passing from **1** to **2**, changes the preferred easy-axis orientation of the $|11/2\rangle$ contribution, moving it to a transverse geometry and predictably lowering the barrier. The diamagnetic Co^{III} ions are revealed to be surprisingly important, in **1**, as they provide a strong positive charge along the pseudo-C_3 axis. This is fundamental in reducing the $|15/2\rangle$ contribution to the ground state, as the highest m_j state is predicted to be preferentially oriented where the negative charge is most dense. Without the Co^{III} ions, the coordinating atoms and Cp^- rings would stabilize a $|15/2\rangle$ ground state (Figures 5c, 5d, S34, S35).

Conclusions

We have rationally used bulky tripodal ligands to obtain a nearly-ideal octahedral geometry around rare-earths, resulting in two new Dy^{III} SMMs. We have subjected them to a detailed experimental and theoretical magnetic analysis. By combining the REC-model (an effective point-charge approach) and the CONDON software (using the full Hamiltonian), it has been possible to theoretically simulate the magnetic anisotropy, including the susceptibility along three perpendicular rotations. Furthermore, using these considerations, we could rationalize the role of the different constituents of the molecule, including the diamagnetic Co^{III} ions, which provide a strong positive charge along the pseudo-C_3 axis, making it the main magnetic axis in spite of the near-octahedral coordination sphere.

ASSOCIATED CONTENT

Supporting Information. X-ray crystallographic files in CIF format, additional structural, magnetic data for the complexes. This material is available free of charge via the Internet at http://pubs.acs.org.

AUTHOR INFORMATION

Corresponding Author

*E-mail:lapo.bogani@materials.ox.ac.uk, alejandro.gaita@uv.es and cshong@korea.ac.kr

Authors contributions

The manuscript was written through contributions of all authors. All authors have given approval to the final version of the manuscript.

[&]These authors contributed equally.

ACKNOWLEDGMENT

We thank financial support from Korean Basic Science Research Program (NRF-2015R1A2A1A10055658), KCRC grant (NRF-2012-0008901), Korean Priority Research Centers Program (NRF2010-0020209), EU (ERC-CoG-647301 DECRESIM, ERC-StG-338258 OptoQMol and COST Action 15128 MOLSPIN), the Spanish MINECO (grant MAT2014-56143-R, CTQ2014-52758-P and Excellence Unit María de Maeztu MDM-2015-0538), and the Generalitat Valenciana

(Prometeo Programme of excellence). A.G.-A. acknowledges funding by the MINECO (Ramón y Cajal contract).

REFERENCES

1. (a) Ishikawa, N.; Sugita, M.; Ishikawa, T.; Koshihara, S.-y.; Kaizu, Y., Lanthanide Double-Decker Complexes Functioning as Magnets at the Single-Molecular Level. *J. Am. Chem. Soc.* **2003,** *125*, 8694-8695; (b) Ishikawa, N.; Sugita, M.; Ishikawa, T.; Koshihara, S.-y.; Kaizu, Y., Mononuclear Lanthanide Complexes with a Long Magnetization Relaxation Time at High Temperatures: A New Category of Magnets at the Single-Molecular Level. *J. Phy. Chem. B* **2004,** *108*, 11265-11271.

2. (a) Woodruff, D. N.; Winpenny, R. E.; Layfield, R. A., Lanthanide single-molecule magnets. *Chem. Rev.* **2013,** *113* (7), 5110-5148; (b) Liddle, S. T.; van Slageren, J., Improving f-element single molecule magnets. *Chem. Soc. Rev.* **2015,** *44* (19), 6655-6669; (c) Gregson, M.; Chilton, N. F.; Ariciu, A.-M.; Tuna, F.; Crowe, I. F.; Lewis, W.; Blake, A. J.; Collison, D.; McInnes, E. J. L.; Winpenny, R. E. P.; Liddle, S. T., A monometallic lanthanide bis(methanediide) single molecule magnet with a large energy barrier and complex spin relaxation behaviour. *Chem. Sci.* **2016,** *7* (1), 155-165; (d) Chen, Y. C.; Liu, J. L.; Ungur, L.; Liu, J.; Li, Q. W.; Wang, L. F.; Ni, Z. P.; Chibotaru, L. F.; Chen, X. M.; Tong, M. L., Symmetry-Supported Magnetic Blocking at 20 K in Pentagonal Bipyramidal Dy(III) Single-Ion Magnets. *J. Am. Chem. Soc.* **2016,** *138* (8), 2829-2837; (e) Liu, J.; Chen, Y. C.; Liu, J. L.; Vieru, V.; Ungur, L.; Jia, J. H.; Chibotaru, L. F.; Lan, Y.; Wernsdorfer, W.; Gao, S.; Chen, X. M.; Tong, M. L., A Stable Pentagonal Bipyramidal Dy(III) Single-Ion Magnet with a Record Magnetization Reversal Barrier over 1000 K. *J. Am. Chem. Soc.* **2016,** *138* (16), 5441-5450; (f) Coutinho, J. T.; Antunes, M. A.; Pereira, L. C.; Bolvin, H.; Marcalo, J.; Mazzanti, M.; Almeida, M., Single-ion magnet behaviour in [U(Tp(Me$_2$))$_2$I]. *Dalton Trans.* **2012,** *41* (44), 13568-13571.

3. (a) Martínez-Pérez, M. J.; Cardona-Serra, S.; Schlegel, C.; Moro, F.; Alonso, P. J.; Prima-García, H.; Clemente-Juan, J. M.; Evangelisti, M.; Gaita-Arino, A.; Sesé, J.; van Slageren, J.; Coronado, E.; Luis, F., Gd-based single-ion magnets with tunable magnetic anisotropy: molecular design of spin qubits. *Phys. Rev. Lett.* **2012,** *108* (24), 247213; (b) Luis, F.; Repollés, A.; Martínez-Pérez, M. J.; Aguilà, D.; Roubeau, O.; Zueco, D.; Alonso, P. J.; Evangelisti, M.; Camón, A.; Sesé, J.; Barrios, L. A.; Aromí, G., Molecular prototypes for spin-based CNOT and SWAP quantum gates. *Phys. Rev. Lett.* **2011,** *107* (11), 117203; (c) Baldoví, J. J.; Cardona-Serra, S.; Clemente-Juan, J. M.; Coronado, E.; Gaita-Ariño, A.; Prima-Garcia, H., Coherent manipulation of spin qubits based on polyoxometalates: the case of the single ion magnet [GdW$_{30}$P$_5$O$_{110}$]$_{14}$. *Chem. Commun.* **2013,** *49* (79), 8922-8924; (d) Baldoví, J. J.; Cardona-Serra, S.; Clemente-Juan, J. M.; Coronado, E.; Gaita-Ariño, A.; Palii, A., Rational design of single-ion magnets and spin qubits based on mononuclear lanthanoid complexes. *Inorg. Chem.* **2012,** *51* (22), 12565-12574; (e) Shiddiq, M.; Komijani, D.; Duan, Y.; Gaita-Arino, A.; Coronado, E.; Hill, S., Enhancing coherence in molecular spin qubits via atomic clock transitions. *Nature* **2016,** *531* (7594), 348-351; (f) Thiele, S.; Balestro, F.; Ballou, R.; Klyatskaya, S.; Ruben, M.; Wernsdorfer, W., Electrically driven nuclear spin resonance in single-molecule magnets. *Science* **2014,** *344* (6188), 1135-1138.

4. (a) Ding, Y.-S.; Chilton, N. F.; Winpenny, R. E. P.; Zheng, Y.-Z., On Approaching the Limit of Molecular Magnetic Anisotropy:A Near-Perfect Pentagonal Bipyramidal Dysprosium(III)Single-Molecule Magnet. *Angew. Chem. Int. Ed.* **2016**, DOI: 10.1002/anie.201609685; (b) Zadrozny, J. M.; Niklas, J.; Poluektov, O. G.; Freedman, D. E., Millisecond Coherence Time in a Tunable Molecular Electronic Spin Qubit. *ACS Cent. Sci.* **2015,** *1* (9), 488-492.

5. Atzori, M.; Morra, E.; Tesi, L.; Albino, A.; Chiesa, M.; Sorace, L.; Sessoli, R., Quantum Coherence Times Enhancement in Vanadium(IV)-based Potential Molecular Qubits: the Key Role of the Vanadyl Moiety. *J. Am. Chem. Soc.* **2016,** *138* (35), 11234-11244.

6. (a) Clemente-Juan, J. M.; Coronado, E.; Gaita-Ariño, A., Magnetic polyoxometalates: from molecular magnetism to molecular spintronics and quantum computing. *Chem. Soc. Rev.* **2012,** *41* (22), 7464-7478; (b) Cardona-Serra, S.; Clemente-Juan, J. M.; Coronado, E.; Gaita-Ariño, A.; Camón, A.; Evangelisti, M.; Luis, F.; Martínez-Peréz, M. J.; Sesé, J., Lanthanoid single-ion magnets based on polyoxometalates with a 5-fold symmetry: the series [LnP$_5$W$_{30}$O$_{110}$]$^{12-}$ (Ln3+ = Tb, Dy, Ho, Er, Tm, and Yb). *J. Am. Chem. Soc.* **2012,** *134* (36), 14982-14990.

7. Chilton, N. F.; Collison, D.; McInnes, E. J.; Winpenny, R. E.; Soncini, A., An electrostatic model for the determination of magnetic anisotropy in dysprosium complexes. *Nat. Commun.* **2013,** *4*, 2551.

8. (a) Zhang, P.; Guo, Y.-N.; Tang, J., Recent advances in dysprosium-based single molecule magnets: Structural overview and synthetic strategies. *Coord. Chem. Rev.* **2013,** *257* (11-12), 1728-1763; (b) Qian, K.; Baldoví, J. J.; Jiang, S.-D.; Gaita-Ariño, A.; Zhang, Y.-Q.; Overgaard, J.; Wang, B.-W.; Coronado, E.; Gao, S., Does the thermal evolution of molecular structures critically affect the magnetic anisotropy? *Chem. Sci.* **2015,** *6* (8), 4587-4593.

9. (a) Jiang, S. D.; Wang, B. W.; Su, G.; Wang, Z. M.; Gao, S., A mononuclear dysprosium complex featuring single-molecule-magnet behavior. *Angew. Chem. Int. Ed.* **2010,** *49* (41), 7448-7451; (b) Bi, Y.; Guo, Y. N.; Zhao, L.; Guo, Y.; Lin, S. Y.; Jiang, S. D.; Tang, J.; Wang, B. W.; Gao, S., Capping ligand perturbed slow magnetic relaxation in dysprosium single-ion magnets. *Chem. Eur. J.* **2011,** *17* (44), 12476-124781; (c) Li, D. P.; Wang, T. W.; Li, C. H.; Liu, D. S.; Li, Y. Z.; You, X. Z., Single-ion magnets based on mononuclear lanthanide complexes with chiral Schiff base ligands [Ln(FTA)$_3$L] (Ln = Sm, Eu, Gd, Tb and Dy). *Chem. Commun.* **2010,** *46* (17), 2929-2931; (d) Wang, H.; Wang, K.; Tao, J.; Jiang, J., Twist angle perturbation on mixed (phthalocyaninato)(porphyrinato) dysprosium(III) double-decker SMMs. *Chem. Commun.* **2012,** *48* (24), 2973-2975; (e) Chen, G. J.; Guo, Y. N.; Tian, J. L.; Tang, J.; Gu, W.; Liu, X.; Yan, S. P.; Cheng, P.; Liao, D. Z., Enhancing anisotropy barriers of dysprosium(III) single-ion magnets. *Chem. Eur. J.* **2012,** *18* (9), 2484-2487.

10. Baldoví, J. J.; Rosaleny, L. E.; Ramachandran, V.; Christian, J.; Dalal, N. S.; Clemente-Juan, J. M.; Yang, P.; Kortz, U.; Gaita-Ariño, A.; Coronado, E., Molecular spin qubits based on lanthanide ions encapsulated in cubic

polyoxopalladates: design criteria to enhance quantum coherence. *Inorg. Chem. Front.* **2015,** *2*, 893-897.

11. Shiddiq, M.; Komijani, D.; Duan, Y.; Gaita-Ariño, A.; Coronado, E.; Hill, S., Enhancing coherence in molecular spin qubits via atomic cloc transitions. *Nature* **2016**, *531*, 348-351.

12. Jenkins, M. D.; Duan, Y.; Diosdado, B.; García-Ripoll, J. H.; Gaita-Ariño, A.; Giménez-Saiz, C.; Alonso, P. J.; Coronado, E.; Luis, F. Coherent manipulation of three-quit states in a molecular single-ion magnet. *Phys. Rev. B* **2017**, *95*, 064423.

13. Liu, J.-L.; Chen, Y.-C.; Zheng, Y.-Z.; Lin, W.-Q.; Ungur, L.; Wernsdorfer, W.; Chibotaru, L. F.; Tong, M.-L., Switching the anisotropy barrier of a single-ion magnet by symmetry change from quasi-D_{5h} to quasi-O_h. *Chem. Sci.* **2013**, *4*, 3310-3316.

14. (a) Zeng, D.; Ren, M.; Bao, S.-S.; Li, L.; Zheng, L.-M. A luminescent heptanuclear $DyIr_6$ complex showing field-induced slow magnetization relaxation. *Chem. Commun.* **2014**, *50*, 8356-8359. (b) König, S. N.; Chilton, N. F.; Maichle-Mössmer, C.; Pineda, E. M.; Pugh, T.; Anwander, R.; Layfield, R. A. Fast magnetic relaxation in an octahedral dysprosium tetramethyl-aluminate complex. *Dalton Trans.* **2014**, *43*, 3035-3038. (c) Klementyeva, S. V.; Afonin, M. Y.; Bogomyakov, A. S.; Gamer, M. T.; Roesky, P. W.; Konchenko, S. K. Mono- and Dinuclear Rare-Earth Chlorides Ligated by a Mesityl0Substituted β-Diketiminate. *Eur. J. Inorg. Chem.* **2016**, 3666-3672.

15. (a) Kläui, W.; Eberspach, W.; Gütlich, P., Spin-Crossover Cobalt (III) Complexes: Steric and Electronic Control of Spin State. *Inorg. Chem.* **1987,** *26*, 3977-3982; (b) Kläui, W.; Eberspach, W.; Schwarz, R., ZUR REAKTIVITÄT VON COBALTOCEN UND NICKELOCEN GEGENÜBER SEKUNDÄREN PHOSPHINCHALKOGENIDEN: EIN WEG ZU MEHRZÄHNIZEN SAUERSTOFF-UND SCHWEFEL-LIGANDEN. *J. Organomet. Chem.* **1983,** *252*, 347-357.

16. (a) van Leusen, J.; Speldrich, M.; Schilder, H.; Kögerler, P., Comprehensive insight into molecular magnetism via CONDON: Full vs. effective models. *Coord. Chem. Rev.* **2015,** *289-290*, 137-148; (b) Speldrich, M.; Schilder, H.; Lueken, H.; Kögerler, P., A Computational Framework for Magnetic Polyoxometalates and Molecular Spin Structures: CONDON 2.0. *Isr. J. Chem.* **2011,** *51*, 215-227.

17. Baldoví, J. J.; Borrás-Almenar, J. J.; Clemente-Juan, J. M.; Coronado, E.; Gaita-Ariño, A., Modeling the properties of lanthanoid single-ion magnets using an effective point-charge approach. *Dalton Trans.* **2012,** *41* (44), 13705-13710.

18. Baldoví, J. J.; Cardona-Serra, S.; Clemente-Juan, J. M.; Coronado, E.; Gaita-Ariño, A.; Palii, A., SIMPRE: A software package to calculate crystal field parameters, energy levels, and magnetic properties on mononuclear lanthanoid complexes based on charge distributions. *J. Comput. Chem.* **2013,** *34* (22), 1961-1967.

19. Drew, M. G. B.; Harding, C. J.; McKee, V.; Morgan, G. G.; Nelson, J., Geometric Control of Manganese Redox State. *J. Chem. Soc., Chem. Commun.* **1995**, 1035-1038.

20. Alvarez, S.; Alemany, P.; Casanova, D.; Cirera, J.; Llunell, M.; Avnir, D., Shape maps and polyhedral interconversion paths in transition metal chemistry. *Coord. Chem. Rev.* **2005,** *249* (17-18), 1693-1708.

21. (a) Sutter, J.-P.; Kahn, M. L.; Kahn, O., Conclusive Demonstration of the Ferromagnetic Nature of the Interaction Between Holmium(III) and Aminoxyl Radicals. *Adv. Mater.* **1999,** *11*, 863-865; (b) Kahn, M. L.; Sutter, J.-P.; Golhen, S.; Guionneau, P.; Ouahab, L.; Kahn, O.; Chasseau, D., Systematic Investigation of the Nature of The Coupling between a Ln(III) Ion (Ln) Ce(III) to Dy(III)) and Its Aminoxyl Radical Ligands. Structural and Magnetic Characteristics of a Series of {Ln(organic radical)$_2$} Compounds and the Related {Ln(Nitrone)$_2$} Derivatives. *J. Am. Chem. Soc.* **2000,** *122*, 3413-3421.

22. (a) Tang, J.; Hewitt, I.; Madhu, N. T.; Chastanet, G.; Wernsdorfer, W.; Anson, C. E.; Benelli, C.; Sessoli, R.; Powell, A. K., Dysprosium triangles showing single-molecule magnet behavior of thermally excited spin states. *Angew. Chem. Int. Ed.* **2006,** *45* (11), 1729-1733; (b) Layfield, R. A.; McDouall, J. J.; Sulway, S. A.; Tuna, F.; Collison, D.; Winpenny, R. E., Influence of the N-bridging ligand on magnetic relaxation in an organometallic dysprosium single-molecule magnet. *Chem. Eur. J.* **2010,** *16* (15), 4442-4446; (c) Gamer, M. T.; Lan, Y.; Roesky, P. W.; Powell, A. K.; Clérac, R., Pentanuclear Dysprosium Hydroxy Cluster Showing Single-Molecule-Magnet Behavior. *Inorg. Chem.* **2008,** *47*, 6581-6583; (d) Zheng, Y.-Z.; Lan, Y.; Anson, C. E.; Powell, A. K., Anion-Perturbed Magnetic Slow Relaxation in Planar {Dy_4} Clusters. *Inorg. Chem.* **2008,** *47*, 10813-10815.

23. (a) Blagg, R. J.; Tuna, F.; McInnes, E. J.; Winpenny, R. E., Pentametallic lanthanide-alkoxide square-based pyramids: high energy barrier for thermal relaxation in a holmium single molecule magnet. *Chem. Commun.* **2011,** *47* (38), 10587-10589; (b) Koo, B. H.; Lim, K. S.; Ryu, D. W.; Lee, W. R.; Koh, E. K.; Hong, C. S., A unique tetranuclear $Er(III)_4$ cluster exhibiting field-induced single-molecule magnetism. *Chem. Commun.* **2012,** *48* (19), 2519-2521; (c) Sorace, L.; Benelli, C.; Gatteschi, D., Lanthanides in molecular magnetism: old tools in a new field. *Chem. Soc. Rev.* **2011,** *40* (6), 3092-3104; (d) Jiang, S. D.; Wang, B. W.; Sun, H. L.; Wang, Z. M.; Gao, S., An organometallic single-ion magnet. *J. Am. Chem. Soc.* **2011,** *133* (13), 4730-4733; (e) Snyder, J.; Ueland, B. G.; Slusky, J. S.; Karunadasa, H.; Cava, R. J.; Mizel, A.; Schiffer, P., Quantum-classical reentrant relaxation crossover in $Dy_2Ti_2O_7$ spin ice. *Phys. Rev. Lett.* **2003,** *91* (10), 107201.

24. (a) Brown, A. J.; Pinkowicz, D.; Saber, M. R.; Dunbar, K. R., A Trigonal-Pyramidal Erbium(III) Single-Molecule Magnet. *Angew. Chem. Int. Ed.* **2015,** *54* (20), 5864-5868; (b) Meihaus, K. R.; Minasian, S. G.; Lukens, W. W., Jr.; Kozimor, S. A.; Shuh, D. K.; Tyliszczak, T.; Long, J. R., Influence of pyrazolate vs N-heterocyclic carbene ligands on the slow magnetic relaxation of homoleptic trischelate lanthanide(III) and uranium(III) complexes. *J. Am. Chem. Soc.* **2014,** *136* (16), 6056-6068.

25. Sievers, J., Asphericity of 4f-Shells in Their Hund's Rule Ground States. *Z. Phys. B Cond. Mat.* **1982,** *45*, 289-296.

Custom Coordination Environments for Lanthanoids: Tripodal Ligands Achieve Near-Perfect Octahedral Coordination for Two Dy-Based Molecular Nanomagnets

K.S. Lim, J.J. Baldoví, S.D. Jiang, B.H. Koo, D.W. Kang, W.R. Lee, E.K. Koh, A.Gaita-Ariño*, E. Coronado, M. Slota, L. Bogani*, and C.S. Hong*

We present the synthesis, magnetic properties and modelling of two new Dy complexes with octahedral symmetry around the rare-earth. We show that the magnetic behaviour can be interpreted with electrostatic models, providing a first connection with the ligand-field theory used in transition metal ions. Using the methodology we extract structure-properties correlations and provide directions for the rational tuning of magnetic rare-earths complexes.